The application of automated feedback and feedforward control to a LED-based photocatalytic reactor

Khodadadian, Maryam; Galnares de la Garza, F.O.; van Ommen, Ruud; Stankiewicz, Andrzej; Lakerveld, Richard

DOI
10.1016/j.cej.2018.12.134

Publication date
2019

Document Version
Final published version

Published in
Chemical Engineering Journal

The Application of Automated Feedback and Feedforward Control to a LED-based Photocatalytic Reactor

Fatemeh Khodadadian[a], Francisco Galnares de la Garza[a], J. Ruud van Ommen[b], Andrzej I. Stankiewicz[a], Richard Lakerveld[c,*]

[a] Department of Process & Energy, Delft University of Technology, Leeghwaterstraat 39, 2628 CB, Delft, the Netherlands

[b] Chemical Engineering Department, Delft University of Technology, Van der Maasweg 9, 2629 HZ Delft, The Netherlands

[c] Department of Chemical and Biological Engineering, The Hong Kong University of Science & Technology, Clear Water Bay, Kowloon, Hong Kong

* Corresponding author: kelakerveld@ust.hk, Tel.: +852 3469 2217

Abstract

An optimal photon utilization is important for the economic performance of a photocatalytic reactor. However, for the desired reactor performance, it is often difficult to predict the required photon utilization. In this work, automated feedback and feedforward controllers are investigated to maintain the reactor conversion close to a desired value by adjusting the photon irradiance within a LED-based photocatalytic reactor for toluene degradation. The feedback controller was able to control the conversion during a set-point tracking experiment and was able to mitigate the effects of catalyst deactivation in an automated fashion. The feedforward controller was designed based on an empirical steady-state model to mitigate the effect of changing toluene inlet concentration and relative humidity, which were measured input disturbances. The results demonstrated that feedback and feedforward control were complementary and could mitigate the effects of disturbances effectively such that the photocatalytic reactor operated close to desired conditions at all times. The presented work is the first example of how online analytical technologies can be combined with "smart" light sources such as LEDs to implement automated process control loops that optimize photon utilization. Future work may expand on this concept by developing more advanced control strategies and exploring applications in different areas.

Keywords: photocatalytic reactors, light emitting diodes, feedback control, feedforward control, light utilization optimization, volatile organic compounds

1. Introduction

Photocatalysis is an attractive process to support a broad range of chemical reactions[1-3]. However, despite many successful demonstrations of applications on a lab-scale, large-scale applications are currently limited due to several challenges that need to be resolved. The efficient utilization of light within a photocatalytic reactor is one such challenge, which affects the economic feasibility when using artificial light sources.

Efficient utilization of light depends on several factors including the reactor design, the light source, as well as operating conditions. An efficient reactor design should optimize the interplay between mass transfer and photon transfer[4, 5]. The optimal design of photocatalytic reactors has been studied extensively and different designs have been proposed for various applications involving gas and liquid phases [6-8]. The light source itself also plays an important role in the overall efficiency of a photocatalytic process. Conventional UV lamps such as mercury and xenon lamps have been used for different applications. However, drawbacks related to the toxic disposal, short lifetime, fragility, potential for gas leakage, and low efficiency have triggered the exploration of alternative light sources such as light emitting diodes (LEDs)[9-12]. Compared to conventional UV lamps, LEDs offer several advantages when used within a photocatalytic reactor. In addition to their non-toxicity, potential to reduce costs, robustness, longer lifetime, and higher efficiency, LEDs also provide more degrees of freedom for the design of a photocatalytic reactor due to their small size. Furthermore, the illumination intensity of an LED is proportional to the electrical current, which provides opportunities to smartly control the illumination by, for example, employing periodic illumination [13-16] or by creating an optimal illumination profile within a reactor balancing a desired reaction rate while minimizing operating costs. In the design phase, the combination of a spatial light intensity model and a reactor model can be optimized simultaneously to minimize the total costs for equipment and operation[17]. However, during operation, a LED-based photocatalytic reactor may not operate under optimal conditions due to design uncertainty and the presence of external disturbances acting on the system, which may result in a non-optimal energy consumption of the system.

Automated feedback control is a standard solution for continuous flow reactors to compensate for design uncertainty and to reject disturbances acting on the reactor[18-20]. Usually, rather than directly controlling an economic objective function, a set of controlled variables is chosen such that when kept constant, a minimum loss with respect to the economic optimum is obtained, which is referred to as self-optimizing control[21-26]. A main source of operational costs of a photocatalytic reactor involves the energy required for illumination when artificial light sources are used. Generally, a higher light intensity allows for a faster reaction, but the effect will be limited above a certain conversion. Furthermore, for some applications, only conversion above a certain value may be needed (e.g., in the case of environmental applications). Therefore, maintaining the conversion at a desired value in a feedback control loop with illumination as a manipulated variable could provide self-optimizing control for a photocatalytic reactor. Due to the emergence of 'smart' light sources such as LEDs and significant improvements in on-line analytical technologies, such self-optimizing control has now become feasible for LED-based photocatalytic reactors. However, to the best of our knowledge, no studies on self-optimizing feedback control for LED-based catalytic reactors exist in literature despite its potential to improve the economic performance of photocatalytic reactors.

The objective of this paper is to demonstrate and characterize automated feedback control for a LED-based photocatalytic reactor. The conversion has been chosen as the controlled variable with the light intensity of the LEDs as a manipulated variable to achieve self-optimizing control in an automated feedback control loop. Furthermore, feedforward control is studied to further improve the performance of the automated control loop. Feedforward control relies on the measurement of a disturbance followed by preventive action to avoid a significant impact on the controlled variable. Since feedforward control has a preventive character and feedback control has a corrective character, a synergistic effect can be achieved through simultaneous application of both control strategies. The photocatalytic oxidation of toluene within an annular LED-based photocatalytic reactor is used as a model system. Toluene is a typical model compound for photocatalytic oxidation studies of volatile organic compounds. Furthermore, toluene is a practically relevant indoor pollutant[27-

30]. Finally, in our earlier work[4], we have studied the kinetics of toluene oxidation in the same reactor, which provides a reference when mimicking challenging conditions for automated process control (e.g., catalyst deactivation). Real–time monitoring of the reactor outlet by on-line gas chromatography enabled the automation of the control loop. The delay of such online measurement is taken into account in the design of the controller. Finally, for the design of a feedforward controller, relative humidity and toluene inlet concentration are used as typical measured disturbances acting on the system.

2. Materials and methods

2.1 Equipment and Operating Procedures

The experimental setup (see Fig. 1. (a)) and the catalyst preparation procedure have been described in detail elsewhere [4] and are summarized here for completeness. The setup consists of an annular LED-based photocatalytic reactor (see Fig. 1. (b)). The catalyst, TiO_2 (P25, Evonic, 0.2 g ± 0.001 g) is coated on a stainless steel sheet. The thickness of the catalyst layer is 25±6 μm, which was measured with a profilometer (Dektak 8 profilometer, Veeco GmbH) at several points on the catalytic sheet. The fraction of the photons that is reflected by the catalytic film was measured as function of wavelength using a spectroradiometer equipped with a 150 mm integrating sphere (Perkin Elmer Lambda 900). For the dominant wavelength used in this study (365 nm), the fraction of light reflected from the catalyst surface is approximately 25%. Therefore, considering that there is no transmission of light in our system, the fraction of light absorbed is approximately 75%. The catalytic sheet is rolled to form a cylinder and placed on the inner wall of the reactor shell. 246 UV LEDs (NSSU100CT, Nichia, Japan) are mounted on the inner cylinder of the reactor to distribute the photons uniformly on the catalytic surface of the inner wall of the outer cylinder. The LEDs have the maximum spectral intensity at 365 nm and 10 nm half height width and a directivity of 55° at 50% of irradiance. A quartz tube separates the LEDs from the reacting medium without interfering with the illumination (see Fig. 1.(b)). The irradiance emitted by the LEDs is manipulated by controlling the current, as the irradiance of the LEDs is proportional to the applied current,

which was achieved by a flexible power supply (Aim TTi model PLH120-P). Depending on the applied current, the power consumption of the LEDs varies from 0.81 to 3.6 W. The corresponding irradiance depends linearly on the applied current with a slope of 113 W m^{-2} mA^{-1}, which was measured by a calibrated spectroradiometer (Avaspec-ULS2048) in the range of 0.030 to 0.12 mA. The reactor inlet is a mixture of nitrogen and oxygen (78vol% and 22vol%, respectively), toluene in the range of 20 to 90 ppm, and water in the range of 0 to 80% relative humidity. The volumetric flow rate of the feed is 1020 ml min^{-1} for all experiments, which corresponds to a residence time of 25s and a laminar flow regime. The reactor operates at 30°C and a back pressure controller maintains the reactor pressure at 1.1bar.

For a typical experiment, first, the reactor feed is led to an on-line gas chromatograph through a bypass line to measure the stable feed composition at the start of each experiment, which is assumed to remain constant during operation. Subsequently, the reactor is purged by introducing the feed mixture to the reactor for 2 hours under dark conditions. Finally, the reactor is illuminated to initiate the photocatalytic reactions. The input of irradiance into the reactor is defined as:

$$E_2 = E_1 + \Delta E_{FC} + \Delta E_{FFC} \quad (1)$$

where E_2 and E_1 are the future and present irradiance of the LEDs in the reactor, respectively. ΔE_{FC} and ΔE_{FFC} are the contributions of feedback control and feedforward control, respectively, designed to maintain the toluene conversion close to the desired set point (X_{sp}).

A part of the reactor effluent is injected into the on-line Gas Chromatograph (GC) (GC-7890B, Agilent Technologies) at a constant flow rate, measured with a Mass Flow Meter (MFM, F-201CV-1K0-RAD, Bronkhorst, The Netherlands), and the rest of the reactor effluent is directed to a vent. The GC is equipped with a methane convertor, two Flame Ionization Detectors (FID, one for hydrocarbons and another one for CO_2 concentrations lower than 50 ppm detection) and two Thermal Conductivity Detectors (TCD, one for N_2 and O_2 and another one for CO_2 detection). In order to facilitate the implementation of automated controllers, a control interface (LabVIEW 2016) has been developed

to collect all the operating conditions. The feedback and feedforward controllers are implemented via built-in functions of LabVIEW for real-time control applications. Finally, the control interface allows for archiving of the process variables for performance characterization.

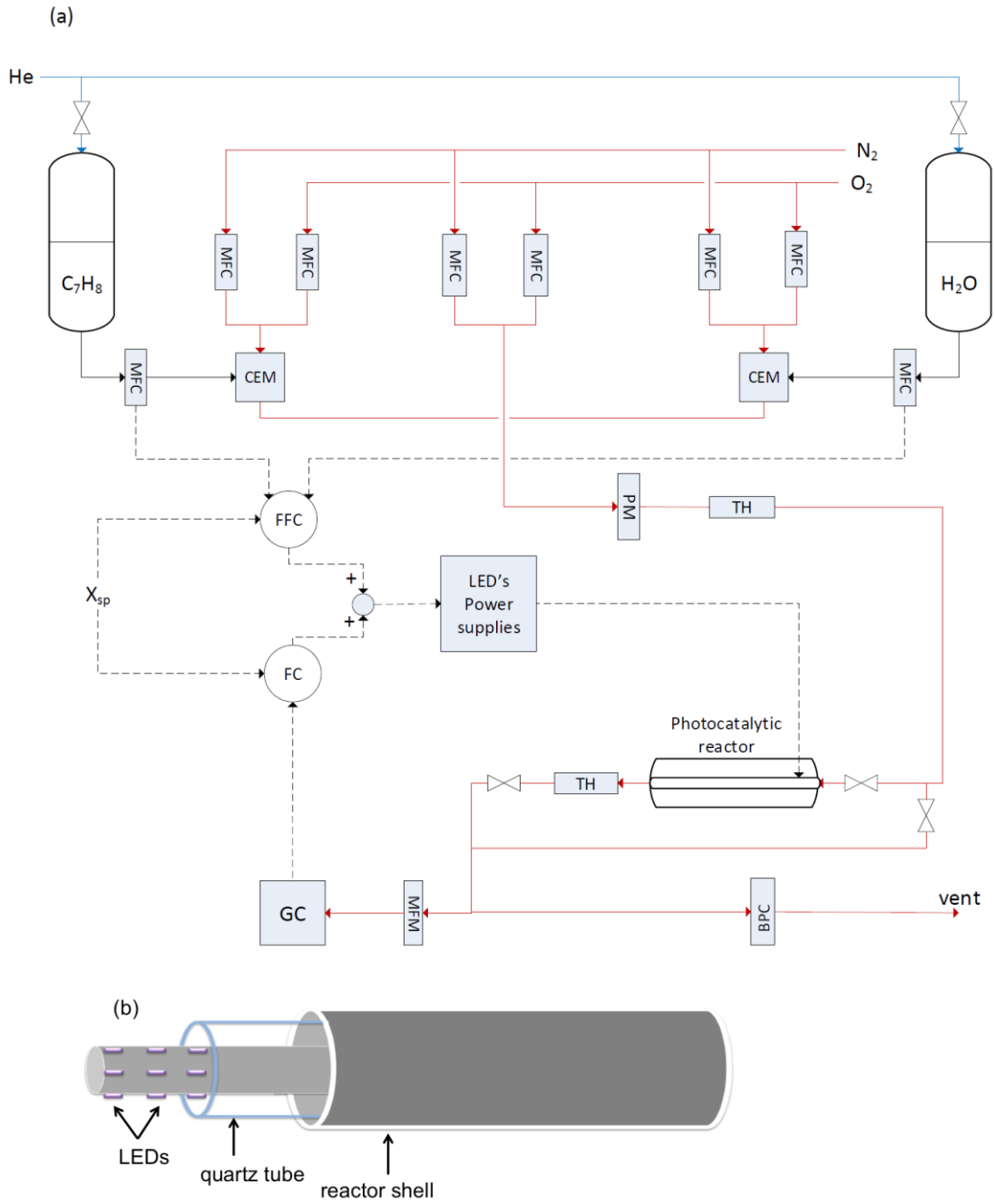

Fig. 1 (a) Flow diagram of the experimental setup. MFC – Mass Flow Controller; BPC- Back Pressure Controller; CEM – Controlled Evaporator Mixer; TH- Thermo Hygrometer; PM- Pressure meter; FC- Feedback Controller; FFC-Feedforward Controller;(b) the structure of the photocatalytic reactor.

To validate the performance of the feedback controller in achieving and maintaining a certain set point, two different sets of experiments were

conducted. In the first set of experiments, at constant toluene inlet concentration (C_t) of 40 ppm and relative humidity (RH) of 60%, the irradiance was manipulated to track different set points.

Our previous study revealed that the ratio of water to toluene inlet concentration plays a significant role in the catalyst deactivation[4]. Water molecules react with the intermediate reaction species, which are accumulated on the catalyst surface, to remove them from that surface in the form of CO_2. Therefore, if the ratio of the water to toluene concentration at the inlet is not sufficiently high, catalyst deactivation becomes significant. Feedback control has the ability to adjust the system automatically to maintain a constant conversion in the presence of catalyst deactivation. Therefore, in the second set of experiments, the feedback controller performance was studied under conditions where catalyst deactivation is expected to be significant. In particular, an experiment at a RH of 40% and a toluene inlet concentration of 40 ppm was conducted to create such conditions.

Catalyst deactivation is an example of an unmeasured disturbance, which has to be rejected with feedback control. In contrast, measured disturbances can be rejected with feedforward control. The RH and toluene concentration at the inlet of the reactor are examples of measured disturbances in our system. Therefore, in the last part of this study, the ability of a combined feedback and forward control system to reject measured and unmeasured disturbances was investigated. To support the design of the feedforward controllers, the dynamic response of the system was studied when step changes in toluene inlet concentration and relative humidity were present in open-loop mode. First, the toluene conversion was monitored at constant toluene inlet concentration (40 ppmv), relative humidity (40%) and irradiance (6.5 Wm^{-2}). Subsequently, a step change in relative humidity from 40% to 60% was implemented. Finally, a step change in toluene inlet concentration from 40 ppmv to 30 ppmv was implemented. The same sequence of step changes was implemented in a separate experiment in closed-loop mode with feedback control only and in closed-loop mode with combined feedback and feedforward control. The operating conditions of all experiments are given in Table 1.

Table 1. The operating conditions of all experiments

ID	RH [%]	C_t [ppmv]	X_{sp} [%]	Irradiance [W m^{-2}]	Controller mode
#1	60	40	40→ 50→ 60→ 30	manipulated variable	closed-loop (feedback)
#2	40	40	40	manipulated variable	closed-loop (feedback)
#3	40 (0-100 min.)	40 (0-100 min.)	-	6.6	Open-loop
	55 (100-200 min.)	40 (100-200 min.)			
	55 (200-end min.)	30 (200-320 min.)			
#4	40 (0-100 min.)	40 (0-100 min.)	30	manipulated variable	closed-loop (feedback)
	55 (100-200 min.)	40 (100-200 min.)			
	55 (200-320 min.)	30 (200-320 min.)			
#5	40 (0-100 min.)	40 (0-100 min.)	30	manipulated variable	closed-loop (combined feedback and feedforward)
	55 (100-200 min.)	40 (100-200 min.)			
	55 (200-320 min.)	30 (200-320 min.)			

2.2. Controller Design and Tuning

2.2.1. Feedback control

The toluene conversion (X) is the controlled variable and the illumination intensity, E [W m^{-2}], of the LEDs is the manipulated variable in the automated

control loops. The proportional-integral (PI) controller is used as a feedback controller, which has two tuning parameters (i.e., controller gain and time constant). The dynamic input-output behavior of the system has been characterized experimentally to obtain numerical values for those two tuning parameters. In particular, the process gain, time constant and time delay are estimated by comparing the dynamic response of the system around the expected steady state to a first-order-plus-time-delay process model, which is an approximation of the true dynamics of the system[31].

Fig. 2 shows the dynamic development of the toluene conversion when the system is perturbed by a series of step changes in irradiance while keeping other process variables constant. The steady-state conversion increases when increasing the irradiance, which is consistent with earlier findings [4]. A time delay of approximately 15 minutes can be seen due to the online measurement. Furthermore, after the delay, a fast increase in conversion can be seen followed by a slow decrease in conversion. The increase is due to the change in manipulated variable (i.e., irradiance), which is to be used in the feedback control loop, whereas the latter slow decrease is expected to be the result of catalyst deactivation. The process gain and process time constant are two characteristic parameters that need to be estimated from the experimental data to design the feedback controller. The process gain (K) is obtained from the ratio of the steady-state conversion before and after the step change in manipulated variable is implemented (see Table 2). The average conversion during the last 100 minutes of every step is used to calculate the steady-state conversion. In reality, the reactor has a nonlinear input-output behavior. Therefore, the calculation of the process gain in principle depends on the operating point at which the step change is implemented. However, it can be seen in Table 2 that the process gains calculated from the two different step changes have a similar value. Therefore, a single process gain is used for controller tuning, which is the average of the two process gains.

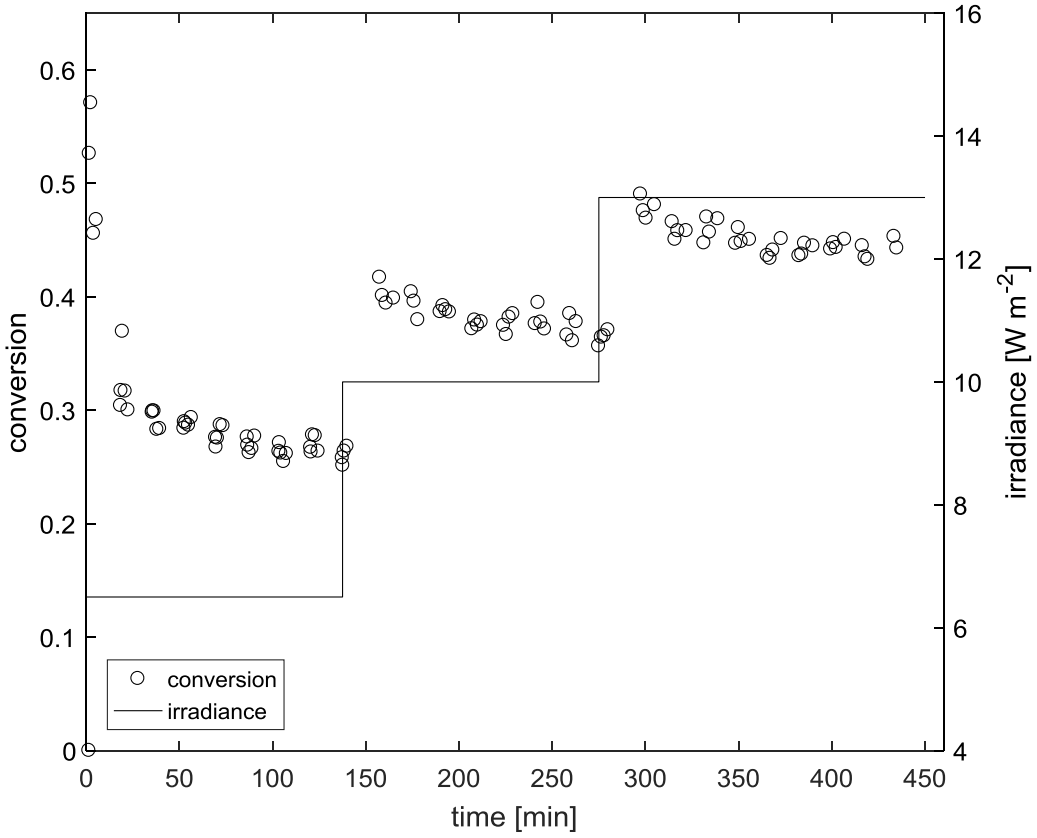

Fig. 2 Dynamic development of the toluene conversion in response to step changes in irradiance. The RH is 60%, toluene inlet concentration is 40 ppmv, and the volumetric flow rate is 1020 ml/min.

Table 2. Average toluene conversion (X) and process gains corresponding to the step changes of irradiance (E)

E_1 [W m^{-2}]	$\bar{X}_1$	E_2 [W m^{-2}]	$\bar{X}_2$	K [m^2 W]
6.5	0.25	10	0.36	0.031
10	0.36	13	0.44	0.027

The process time constant (τ) is obtained by determining the time needed to complete 63% of the transition from the old to the new steady-state conversion, which is difficult to obtain since the response is faster than the sampling period. A more precise determination of the process time constant would require a technical ability to store multiple samples in a short period, which would have to be analysed off-line. However, the aim is to find a value that is order-of-magnitude correct, as feedback control is a model-free control method based on

corrective actions and process delay time is the dominating time constant, which will govern controller design. In particular, a value of 6 minutes has been used as an approximation of the true time constant of the system. Subsequently, the tuning parameters of the PI feedback controller can be determined using standard methods such as the Internal Model Control (IMC) tuning method [31-33] used in this work. The feedback controller is implemented in so-called velocity form to avoid integral windup:

$$\Delta E_{FC} = K_C\left[\left(e_k - e_{k-1}\right) + \frac{\Delta t}{\tau_I} e_k\right], \quad (2)$$

where K_c is the controller gain and τ_I is the integral time. The desired closed–loop time constant has been chosen to be equal to the process time delay [32]. In addition, Δt is the sampling period and e_k is the measured error at the k_{th} sampling instant. The error is defined as the difference between the set point conversion (X_{sp}) and the measured conversion. The calculated irradiance is converted to an electrical current in the final control element of the LEDs, using a linear relation, which was obtained empirically in previous work [17].

2.2.2. Feedforward control

Feedforward control relies on a process model that can predict the impact of a measured disturbance on a controlled variable such that preventive action can be taken to mitigate the impact of the disturbance. Since feedforward control is normally used simultaneously with feedback control, a simple model often suffices, as feedback control can still drive the controlled variable to the desired set point. Therefore, in this work, an empirical steady-state model is used to design the feedforward controller. Typical disturbances for environmental oxidation reactions in the gas phase that have an impact on conversion and that can be measured include the inlet concentration of the organic compound and the relative humidity of the simulated air stream. Both disturbances are used to design the feedforward controller, which will be implemented by adding the outputs of the feedforward and feedback controllers together to calculate the value of the manipulated variable.

In our earlier work [11], the steady-state toluene conversion was experimentally measured as a function of toluene inlet concentration, relative

humidity, volumetric flow rate as well as irradiance at typical operating conditions. For a toluene concentration (C_t) in the range of 20 to 90 ppmv and a relative humidity up to 70%, a volumetric flow rate (Q) of 0.8 to 1.3 l/min and an irradiance of 3 to 13.5 W m^{-2}, the relation between conversion (X_{FFC}) as a function of inlet concentration, and relative humidity is empirically modeled as follows:

$$X_{FFC} = -0.02QC_t(RH)^{1.3} + 0.2E^{0.5} + 0.2 \quad (3)$$

A parity plot (see Fig. 3) shows that the model is reasonably well capable of describing the conversion at steady state for the tested operating conditions despite its simplicity and lack of first principles.

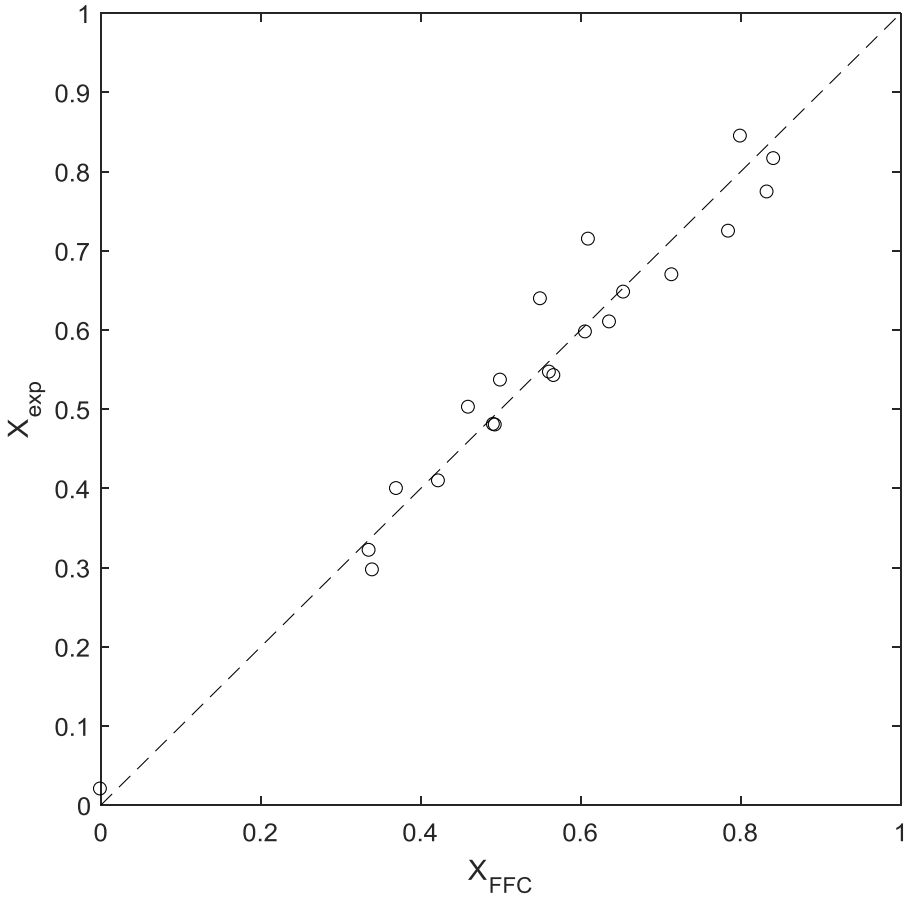

Fig. 3 experimental conversion (X_{exp}) vs. conversion predicted via Eq. (3) (X_{FFC})

From Eq. (3), the anticipated difference in steady-state conversion ($X_{m,\,FFC}$) due to measured changes in inlet concentration and relative humidity can be calculated when assuming negligible changes in volumetric flow rate.

Furthermore, the irradiance to compensate the effect of the disturbance error on the steady-state conversion can also be calculated as below:

$$E_{2,FFC} = \left| E_1^{0.5} + 0.1Q\left(C_{t,2}\left(RH_2\right)^{1.3} - C_{t,1}\left(RH_1\right)^{1.3} \right) \right| \quad (4)$$

where $E_{2,FFC}$ is the irradiance output of the feedforward controller, i.e., the sum of present irradiance (E_1) and the contribution of feedforward control (ΔE_{FFC}).

3. Results & discussion

3.1. Performance characterization of PI feedback control

The conversion and irradiance as a function of time during a set-point tracking experiment with feedback control are illustrated in Fig. 4 (Experiment #1). The data demonstrate that the PI controller is well capable to track set points for conversion within the tested range by using the irradiance as the manipulated variable in an automated fashion. In general, the conversion reaches the set point rapidly without large overshoots or unstable behavior despite the significant measurement delay from the GC.

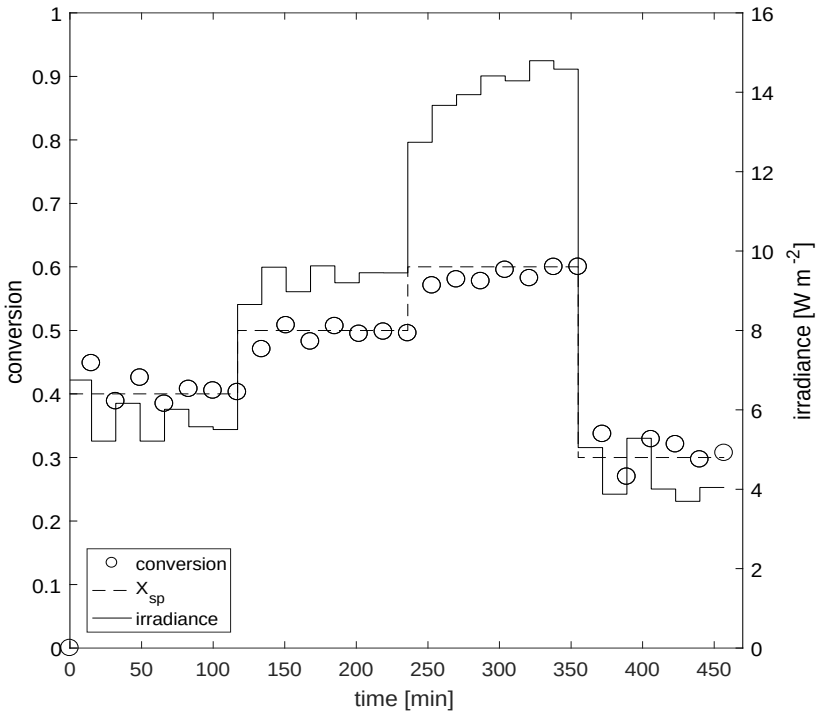

Fig. 4 Dynamic development of the toluene conversion (controlled variable) and irradiance (manipulated variable) during a set-point tracking experiment in closed-loop mode with feedback control (Experiment#1).

Fig. 5 shows the dynamic development of conversion and irradiance during a disturbance-rejection experiment with feedback control (Experiment #2). The data show that the PI controller is well capable to reject the effect of the catalyst deactivation on the conversion at a constant set point. The irradiance increases steadily over time to maintain the conversion close to the desired set point. Therefore, the PI controller is able to optimize the light utilization within the reactor automatically in case substantial catalyst deactivation occurs.

The feedback controllers were designed with commonly used tuning methods, which already yielded satisfactory performance. However, it is expected that further optimization of the controller design would allow for improved closed-loop performance. An investigation into the influence of operational variables such as residence time on the controller design and performance is of interest for future research. The closed-loop time constant is determined by the measurement delay, which is an order of magnitude larger than the space time and several times larger than the estimated process time constant. However, the controller gain should be changed for different operating conditions to account for the nonlinear process behaviour, which is also of interest for future research.

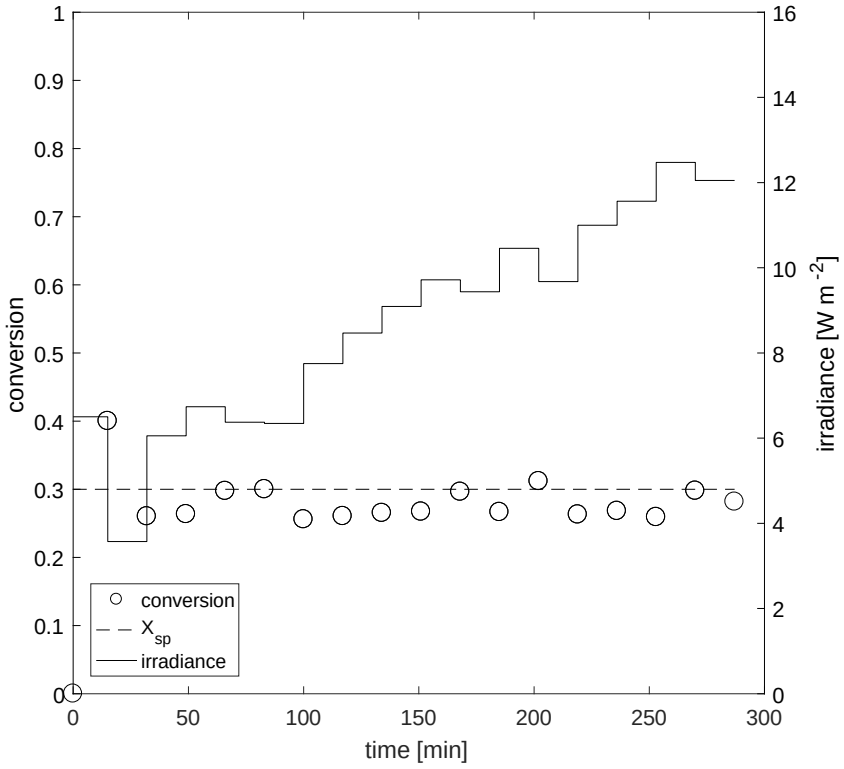

Fig. 5 Dynamic development of the toluene conversion (controlled variable) and irradiance (manipulated variable) during a disturbance-rejection experiment in closed-loop mode with feedback control (Experiment#2).

3.2. Performance characterization of feedback and feedforward control

Fig. 6 demonstrates the dynamic development of the conversion during an open-loop experiment in which the irradiance was kept constant at 6.5 W m^{-2} and the RH of the feed stream was increased after 100 minutes and toluene inlet concentration was decreased after 200 minutes (Experiment #3). The conversion decreased gradually during the first 100 minutes due to the catalyst deactivation, while after the increase in RH from 40 to 60% at 102 minutes, a sharp drop in the conversion from 25% to 18% was observed. Subsequently, the conversion increased gradually over time due to the catalyst regeneration facilitated by the high RH[4]. In the last phase of the experiment, the system was disturbed at 200 minutes by a decrease in toluene concentration from 40 to 30 ppmv and consequently, the conversion showed a further increase over time due to increased catalyst regeneration rate at the higher ratio of water to toluene inlet concentration. The data of the open-loop experiment demonstrate that the

toluene conversion does not remain constant when the inlet water to toluene ratio changes over time. The conversion can be stabilized with feedback control. In addition, since both concentrations are measured, a feedforward controller can be designed to supplement feedback control, as illustrated next.

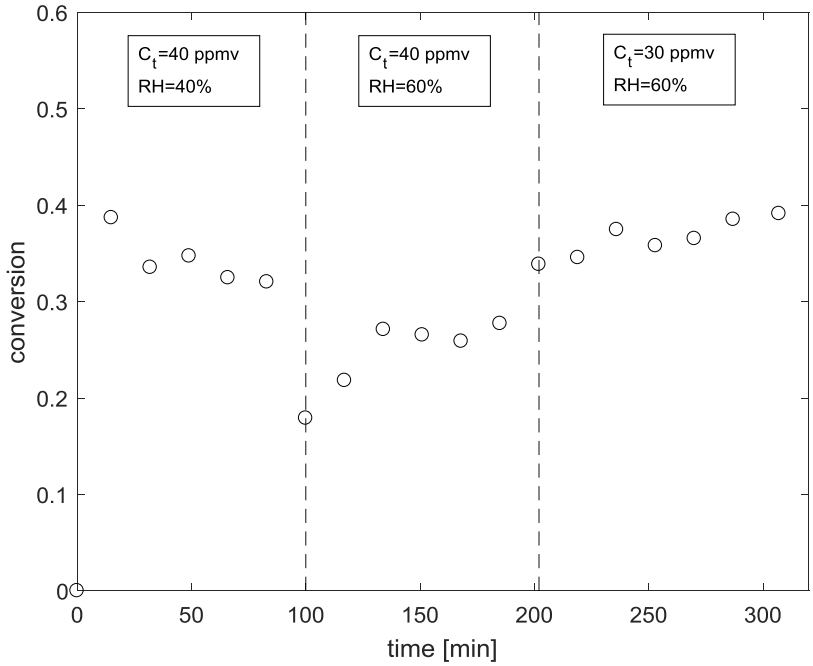

Fig. 6 Toluene conversion during three different operating conditions at a constant irradiance of 6.5 [W m-2] and flow rate of 1020[ml min^{-1}] in open-loop mode (Experiment #3).

Figures 7 and 8 show the variation of toluene conversion and irradiance when the same changes in toluene inlet concentration and RH are implemented with feedback control only and with feedback control in combination with feedforward control (Experiment #4 and #5). The irradiance was used in both cases as the manipulated variable in closed-loop mode. In the first 100 minutes, for both cases it can be seen that the controllers were well capable to maintain the conversion close to the desired set point. However, when the first disturbance was introduced after 100 minutes, a distinct difference can be seen. In case of feedback control only (Fig. 7), the conversion dropped below the set point and it took some time before the irradiance had been sufficiently increased to reject the disturbance. In contrast, when feedback control was used in combination with feedforward control, irradiance was increased much more rapidly due to the contribution of feedforward action. Consequently, the toluene

conversion stayed close to the desired set point and the mitigation of the inlet disturbance was much more effective. Subsequently, the irradiance was gradually reduced due to the regeneration of the catalyst at higher RH, which was driven by feedback control, as this trend could be seen for both cases and was not used to design the feedforward controller. A similar behavior could be observed when the second disturbance was introduced after 200 minutes of operation. In this situation, a higher conversion was measured shortly after the disturbance was introduced when only feedback control was used, as it took time to lower the irradiance. In contrast, feedforward control predicted the required lowering of the irradiance, which resulted in much better controller performance. In summary, both control schemes were eventually capable to reject input disturbances. However, the addition of feedforward control resulted in a more effective mitigation of the disturbances due to the combination of impact prediction of the measured disturbances (i.e., feedforward control) and the corrective action of unmeasured disturbances and model uncertainty (i.e., feedback control).

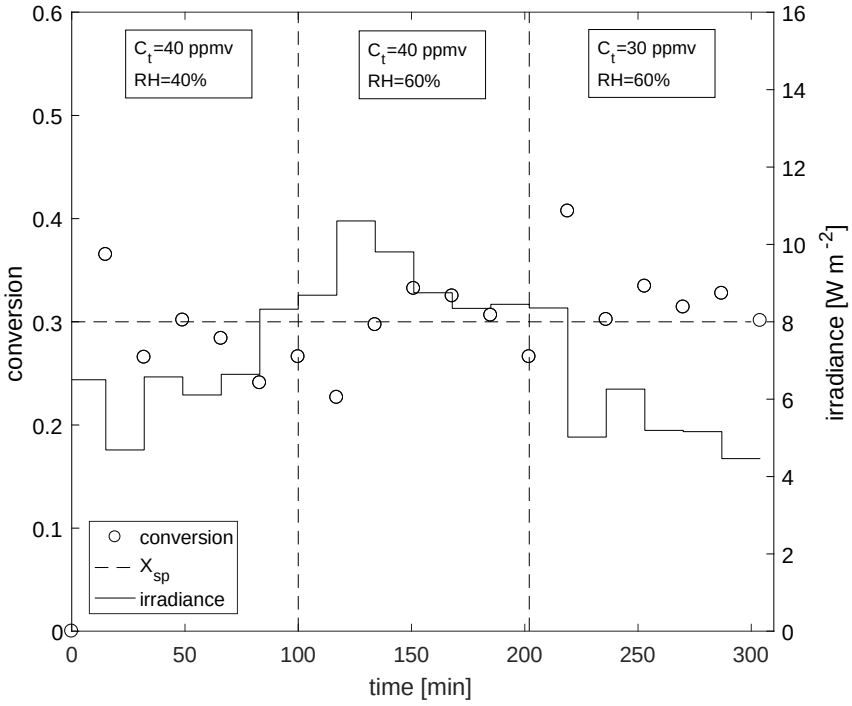

Fig. 7 Toluene conversion (controlled variable) and irradiance (manipulated variable) in closed-loop mode in case of, a) PI feedback controller only (Experiment#4).

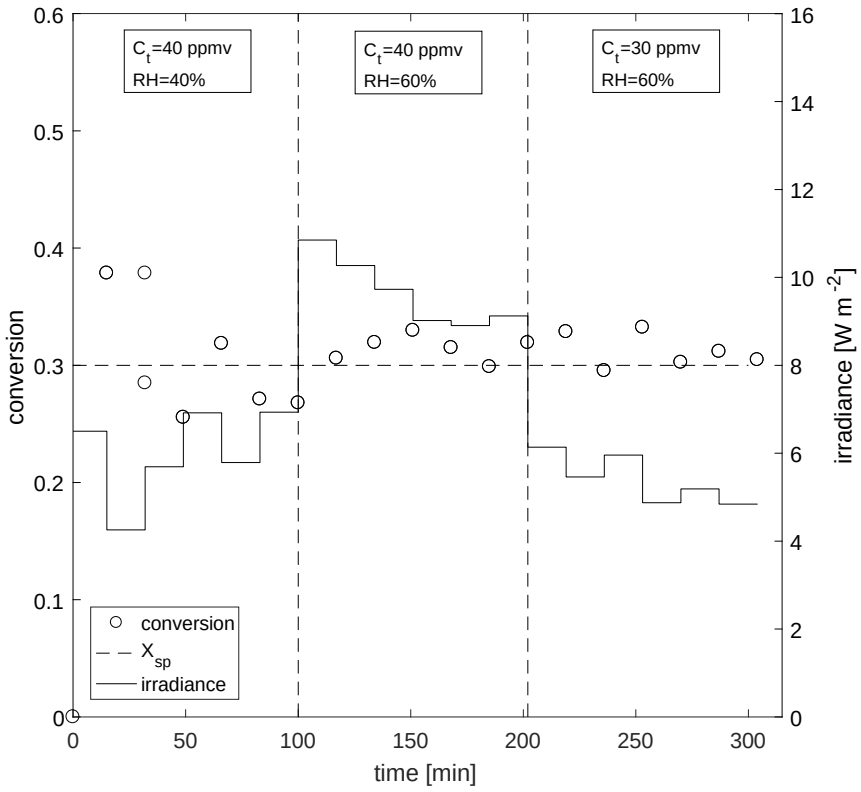

Fig. 8 Toluene conversion (controlled variable) and irradiance (manipulated variable) in closed-loop mode in case of PI feedback controller and feedforward controller (Experiment #5).

4. Conclusion

Online process analytical technologies can be combined with LEDs in automated control loops to maintain the conversion of toluene in a gas-phase photocatalytic reactor close to a desired value in the presence of disturbances. In particular, the experimental results demonstrated that a proportional-integral feedback controller could manipulate the irradiance within the reactor to achieve desired conversions effectively in the presence of disturbances. In case of measured disturbances, such as toluene or water inlet concentrations, the control scheme could be augmented with a feedforward controller based on an empirical steady-state model. A comparison of experiments without any control and with feedback control only demonstrated that feedback control effectively mitigated catalyst deactivation. However, the combined feedback and feedforward control scheme demonstrated superior behavior in case measured disturbances were added to the same set of experiments.

This work demonstrates for the first time how fast online analytical technologies can be combined with “smart” light sources in automated control

loops to maintain the conversion close to a desired value for optimal process operation. Future work may focus on developing more advanced control strategies (e.g., model-predictive control) or exploring other applications.

Acknowledgement

This research is funded by the European Research Council in the framework of the Seventh Framework Programme (FP7) under grant agreement no ERC-2010-AdG-267348. Lennart Middelplaats from Electrical and Mechanical Support Division of Delft University of technology is acknowledged for support with implementation of the controlling system in Matlab and LabVIEW.

References

[1] C. McCullagh, N. Skillen, M. Adams, P.K.J. Robertson, Photocatalytic reactors for environmental remediation: a review, J. Chem. Technol. Biotechnol. 86 (2011) 1002-1017.

[2] A. Fujishima, K. Honda, Electrochemical Photolysis of Water at a Semiconductor Electrode, Nature 238 (1972) 37-38.

[3] A.F. Tooru Inoue, Satoshi Konishi, Kenichi Honda, photoelectrocatalytic reduction of carbon dioxide in aqueus suspension of semiconductor powders, Nature 277 (1979) 2.

[4] F. Khodadadian, M.W. de Boer, A. Poursaeidesfahani, J.R. van Ommen, A.I. Stankiewicz, R. Lakerveld, Design, characterization and model validation of a LED-based photocatalytic reactor for gas phase applications, Chem. Eng. J. 333 (2018) 456-466.

[5] M. Motegh, J.J. Cen, P.W. Appel, J.R. van Ommen, M.T. Kreutzer, Photocatalytic-reactor efficiencies and simplified expressions to assess their relevance in kinetic experiments, Chem. Eng. J. 207 (2012) 607-615.

[6] F. Khodadadian, M. Nasalevich, F. Kapteijn, A.I. Stankiewicz, R. Lakerveld, J. Gascon, CHAPTER 8 Photocatalysis: Past Achievements and Future Trends, Alternative Energy Sources for Green Chemistry, The Royal Society of Chemistry 2016, pp. 227-269.

[7] T. Van Gerven, G. Mul, J. Moulijn, A. Stankiewicz, A review of intensification of photocatalytic processes, Chem. Eng. Process. 46 (2007) 781-789.
[8] R.J. Braham, A.T. Harris, Review of Major Design and Scale-up Considerations for Solar Photocatalytic Reactors, Ind. Eng. Chem. Res. 48 (2009) 8890-8905.
[9] W.-K. Jo, R.J. Tayade, New Generation Energy-Efficient Light Source for Photocatalysis: LEDs for Environmental Applications, Ind. Eng. Chem. Res. 53 (2014) 2073-2084.
[10] M.R. Eskandarian, H. Choi, M. Fazli, M.H. Rasoulifard, Effect of UV-LED wavelengths on direct photolytic and TiO2 photocatalytic degradation of emerging contaminants in water, Chem. Eng. J. 300 (2016) 414-422.
[11] T.S. Natarajan, M. Thomas, K. Natarajan, H.C. Bajaj, R.J. Tayade, Study on UV-LED/TiO2 process for degradation of Rhodamine B dye, Chem. Eng. J. 169 (2011) 126-134.
[12] K. Song, F. Taghipour, M. Mohseni, Microorganisms inactivation by continuous and pulsed irradiation of ultraviolet light-emitting diodes (UV-LEDs), Chem. Eng. J. 343 (2018) 362-370.
[13] E. Korovin, D. Selishchev, A. Besov, D. Kozlov, UV-LED TiO2 photocatalytic oxidation of acetone vapor: Effect of high frequency controlled periodic illumination, Appl. Catal., B 163 (2015) 143-149.
[14] O. Tokode, R. Prabhu, L.A. Lawton, P.K.J. Robertson, Controlled periodic illumination in semiconductor photocatalysis, J. Photochem. Photobiol. A: Chem. (2015).
[15] Y. Ku, S.-J. Shiu, H.-C. Wu, Decomposition of dimethyl phthalate in aqueous solution by UV–LED/TiO2 process under periodic illumination, J. Photochem. Photobiol. A: Chem. 332 (2017) 299-305.
[16] O. Tokode, R. Prabhu, L.A. Lawton, P.K.J. Robertson, The effect of pH on the photonic efficiency of the destruction of methyl orange under controlled periodic illumination with UV-LED sources, Chem. Eng. J. 246 (2014) 337-342.
[17] F. Khodadadian, A. Poursaeidesfahani, Z. Li, J.R. van Ommen, A.I. Stankiewicz, R. Lakerveld, Model-Based Optimization of a Photocatalytic Reactor with Light-Emitting Diodes, Chem. Eng. Technol. 39 (2016) 1946-1954.

[18] M. Barkhordari Yazdi, M.R. Jahed-Motlagh, Stabilization of a CSTR with two arbitrarily switching modes using modal state feedback linearization, Chem. Eng. J. 155 (2009) 838-843.
[19] M.I. Neria-González, R. Martínez-Guerra, R. Aguilar-López, Feedback regulation of an industrial aerobic wastewater plant, Chem. Eng. J. 139 (2008) 475-481.
[20] R. Caetano, M.A. Lemos, F. Lemos, F. Freire, Modeling and control of an exothermal reaction, Chem. Eng. J. 238 (2014) 93-99.
[21] D.C. Fabry, E. Sugiono, M. Rueping, Self-Optimizing Reactor Systems: Algorithms, On-line Analytics, Setups, and Strategies for Accelerating Continuous Flow Process Optimization, Isr. J. Chem. 54 (2014) 341-350.
[22] C. Houben, A.A. Lapkin, Automatic discovery and optimization of chemical processes, Curr. Opin. Chem. Eng. 9 (2015) 1-7.
[23] A.J. Parrott, R.A. Bourne, G.R. Akien, D.J. Irvine, M. Poliakoff, Self-optimizing continuous reactions in supercritical carbon dioxide, Angew. Chem. Int. Ed. 50 (2011) 3788-3792.
[24] V. Sans, L. Porwol, V. Dragone, L. Cronin, A self optimizing synthetic organic reactor system using real-time in-line NMR spectroscopy, Chemical Science 6 (2015) 1258-1264.
[25] D.C. Fabry, E. Sugiono, M. Rueping, Online monitoring and analysis for autonomous continuous flow self-optimizing reactor systems, React. Chem. Eng. 1 (2016) 129-133.
[26] S. Skogestad, Plantwide control: the search for the self-optimizing control structure, J. Process Control 10 (2000) 487-507.
[27] G. Marcì, M. Addamo, V. Augugliaro, S. Coluccia, E. García-López, V. Loddo, G. Martra, L. Palmisano, M. Schiavello, Photocatalytic oxidation of toluene on irradiated TiO2: comparison of degradation performance in humidified air, in water and in water containing a zwitterionic surfactant, J. Photochem. Photobiol. A: Chem. 160 (2003) 105-114.
[28] Z. Pengyi, L. Fuyan, Y. Gang, C. Qing, Z. Wanpeng, A comparative study on decomposition of gaseous toluene by O3/UV, TiO2/UV and O3/TiO2/UV, J. Photochem. Photobiol. A: Chem. 156 (2003) 189-194.

[29] Y.-p. Zhang, R. Yang, Q.-j. Xu, J.-h. Mo, Characteristics of Photocatalytic Oxidation of Toluene, Benzene, and Their Mixture, J. Air Waste Manage. Assoc. 57 (2007) 94-101.
[30] P.C. Yao, S.T. Hang, C.W. Lin, D.H. Hai, Photocatalytic destruction of gaseous toluene by porphyrin-sensitized TiO2 thin films, J. Taiwan Inst. Chem. Eng. 42 (2011) 470-479.
[31] D.E. Rivera, M. Morari, S. Skogestad, Internal model control: PID controller design, Ind. Eng. Chem. Process Des. Dev. 25 (1986) 252-265.
[32] S. Skogestad, Simple analytic rules for model reduction and PID controller tuning, J. Process Control 13 (2003) 291-309.
[33] C.E. Garcia, M. Morari, Internal model control. A unifying review and some new results, Ind. Eng. Chem. Process Des. Dev. 21 (1982) 308-323.

Figure Captions

Fig. 1 (a) Flow diagram of the experimental setup. MFC – Mass Flow Controller; BPC- Back Pressure Controller; CEM – Controlled Evaporator Mixer; TH- Thermo Hygrometer; PM- Pressure meter; FC-Feedback Controller; FFC-Feedforward Controller;(b) the structure of the photocatalytic reactor.

Fig. 2 Dynamic development of the toluene conversion in response to step changes in irradiance. The RH is 60%, toluene inlet concentration is 40 ppmv, and the volumetric flow rate is 1020 ml/min.

Fig. 3 experimental conversion (X_{exp}) vs. conversion predicted via Eq. (3) (X_{FFC})

Fig. 4 Dynamic development of the toluene conversion (controlled variable) and irradiance (manipulated variable) during a set-point tracking experiment in closed-loop mode with feedback control (Experiment#1).

Fig. 5 Dynamic development of the toluene conversion (controlled variable) and irradiance (manipulated variable) during a disturbance-rejection experiment in closed-loop mode with feedback control (Experiment#2).

Fig. 6 Toluene conversion during three different operating conditions at a constant irradiance of 6.5 [W m^{-2}] and flow rate of 1020[ml min^{-1}] in open-loop mode (Experiment #3).

Fig. 7 Toluene conversion (controlled variable) and irradiance (manipulated variable) in closed-loop mode in case of, a) PI feedback controller only (Experiment#4).

Fig. 8 Toluene conversion (controlled variable) and irradiance (manipulated variable) in closed-lo op mode in case of PI feedback controller and feedforward controller (Experiment #5).